Published in final edited form as:
J Immunol. 2010 June 15; 184(12): 7196–7206. doi:10.4049/jimmunol.0901404.

$\alpha_4\beta_1$ Integrin Mediates the Recruitment of Immature Dendritic Cells across the Blood-Brain Barrier during Experimental Autoimmune Encephalomyelitis

Pooja Jain[*,1], **Caroline Coisne**[†,1], **Gaby Enzmann**[†], **Robert Rottapel**[‡], and **Britta Engelhardt**[†]

[*]Department of Microbiology and Immunology and Drexel Institute for Biotechnology and Virology Research, Drexel University College of Medicine, Doylestown, PA 18902 [†]Theodor Kocher Institute, University of Bern, Bern, Switzerland [‡]Ontario Cancer Institute, Toronto Medical Discovery Tower, Toronto, Ontario, Canada

Abstract

Dendritic cells (DCs) within the CNS are recognized to play an important role in the effector phase and propagation of the immune response in experimental autoimmune encephalomyelitis (EAE), a mouse model for multiple sclerosis. However, the mechanisms regulating DC trafficking into the CNS still need to be characterized. In this study, we show by performing intravital fluorescence videomicroscopy of the inflamed spinal cord white-matter microvasculature in SJL mice with EAE that immature, and to a lesser extent, LPS-matured, bone marrow-derived DCs efficiently interact with the CNS endothelium by rolling, capturing, and firm adhesion. Immature but not LPS-matured DCs efficiently migrated across the wall of inflamed parenchymal microvessels into the CNS. Blocking α_4 integrins interfered with the adhesion but not the rolling or capturing of immature and LPS-matured DCs to the CNS microvascular endothelium, inhibiting their migration across the vascular wall. Functional absence of β_1 integrins but not of β_7 integrins or $\alpha_4\beta_7$ integrin similarly reduced the adhesion of immature DCs to the CNS microvascular endothelium, demonstrating that $\alpha_4\beta_1$ but not $\alpha_4\beta_7$ integrin mediates this step of immature DCs interaction with the inflamed blood-brain barrier during EAE. Our study shows that during EAE, especially immature DCs migrate into the CNS, where they may be crucial for the perpetuation of the CNS-targeted autoimmune response. Thus therapeutic targeting of α_4 integrins affects DC trafficking into the CNS and may therefore lead to the resolution of the CNS autoimmune inflammation by reducing the number of CNS professional APCs.

Address correspondence and reprint requests to Prof. Dr. Britta Engelhardt or Dr. Pooja Jain, Theodor Kocher Institute, University of Bern, Freiestr. 1, CH-3012 Bern, Switzerland (B.E.), or Department of Microbiology and Immunology and Drexel Institute for Biotechnology and Virology Research, Drexel University College of Medicine, 3805 Old Easton Road, Doylestown, PA 18902 (P.J.). bengel@tki.unibe.ch or pjain@drexelmed.edu.

[1]P.J. and C.C. contributed equally to this work.

Disclosures

The authors have no financial conflicts of interest.

The online version of this article contains supplemental material.

In multiple sclerosis (MS) and in its animal model experimental autoimmune encephalomyelitis (EAE), circulating neuroantigen-specific T cells gain access to the CNS. Clinical manifestation of EAE does not only require the initial priming of naive autoreactive $CD4^+$ T cells in the peripheral immune system but critically depends on the reactivation of neuroantigen-specific $CD4^+$ T cells within the CNS to develop into Th1 or Th17 effector cells. Thus, once myelin-specific $CD4^+$ T cells have crossed the endothelial blood-brain barrier (BBB), they need to re-encounter their specific Ag in the context of MHC class II molecules on APCs. Within the CNS, initial Ag presentation is likely to occur in the perivascular spaces between the endothelial and glial basement membranes. This is the only compartment in which, in the healthy CNS [besides the choroid plexus and the meningeal spaces (1)], the presence of MHC class II expressing macrophages and dendritic cells (DCs) has been reported in rodents and man (2–4). In contrast, the CNS parenchyma is found to be completely devoid of MHC class II expressing cells.

During ongoing MS and EAE, a substantial accumulation of DCs has been found in the CNS supporting their active participation in the pathophysiology of these diseases. Increased numbers of DCs were also reported in the CSF of MS patients when compared with control (5). Interestingly, CSF DCs showed a maturing or mature phenotype, when compared with blood DCs from the same patients. Additionally, several studies have identified DCs within inflammatory demyelinating lesions of MS patients (2, 6) and in inflammatory lesions in EAE (2, 3, 7).The preponderance of DCs in the perivascular spaces and their close vicinity to invading T cells suggested a role for DCs in local T cell activation toward myelin components in situ (2).

Functional evidence that Ag presentation by DCs within the CNS contributes to induction and perpetuation of neuroinflammation in EAE has been derived from several studies. For example, systemic injection of Flt-3L leads to a substantial increase in the number of DCs in the CNS and enhanced severity of EAE symptoms (2). Further studies demonstrated that myeloid DCs purified from the CNS of mice with established relapsing EAE have the capacity to present endogenous myelin Ags to both preactivated effector myelin-specific T cells and naive T cells and polarize them along encephalitogenic Th1 and Th17 lineages (3, 8). In this context, DCs were shown to be involved in epitope spreading of the myelin-specific T cell response during CNS inflammation (9). A recent study demonstrating that intracerebral injection of myelin Ag-loaded DCs exacerbated or ameliorated the clinical course of EAE, depending on the activations status of the DCs, even suggests that DCs are the rate-limiting factor of neuroinflammation in MS and EAE (10).

The mechanisms, by which DCs accumulate in the CNS under neuroinflammatory conditions, are not well understood. Increased numbers of DCs could be derived by proliferation from CNS resident DCs or from differentiation from parenchymal microglial cells. The reported accumulation of DCs in close vicinity to CNS microvessels in MS and EAE rather suggests, however, that DCs are recruited from the periphery into the CNS. In this case, the endothelial BBB would control DC trafficking into the CNS during EAE and MS. Interestingly, in vitro studies demonstrated that monocytes could migrate across brain microvascular endothelium and differentiate into DCs (11). These findings have been confirmed in vivo by a recent study demonstrating that during EAE circulating

$CD11b^{+}CD62L^{+}Ly6C^{high}$ monocytes were mobilized from the bone marrow (BM) into the bloodstream by a GM-CSF–dependent pathway, migrate across the BBB, and differentiate into CNS DCs and macrophages (12). On the basis of in vitro evidence that DCs themselves can migrate across brain microvascular endothelial cells (13), it remains to be shown whether circulating DCs can cross the BBB during EAE.

In contrast to T cell trafficking across the BBB during EAE (summarized in Ref. 14), the molecular mechanisms underlying the multistep recruitment of circulating DCs across the BBB in vivo have not been investigated. This prompted us to study the trafficking of DCs across the BBB during EAE by means of intravital fluorescence videomicroscopy (IVM) (15). Direct visualization of the inflamed mouse spinal cord white-matter microcirculation allowed us to observe the rolling, capture, and firm adhesion of infused fluorescently labeled DCs within this vascular bed in vivo. Immature but much less so LPS-matured BM-derived DCs effectively initiated contact with the BBB endothelium by rolling and capturing, then firmly adhered to the mouse spinal cord white-matter microvasculature and finally extravasated across the BBB into the CNS. Firm adhesion, but not rolling and capturing, of both immature and LPS-matured DCs to the BBB was mediated by α_4 integrins. Functional absence of β_1 integrins, but not of β_7 integrins or specifically $\alpha_4\beta_7$ integrin, similarly reduced the adhesion of immature DCs to the CNS microvasular endothelium, demonstrating that $\alpha_4\beta_1$ integrin mediates the firm adhesion of immature DCs to the BBB endothelium in EAE.

To the best of our knowledge, our study represents the first live imaging study on DC trafficking across the BBB that demonstrates an involvement of $\alpha_4\beta_1$ integrin in this process. Therapeutic targeting of α_4 integrins in MS may therefore block DC trafficking to the CNS and thus resolve CNS autoimmune inflammation by reducing the number of CNS professional APCs.

Materials and Methods

Mice

Animal experiments were performed in accordance with the legislation on animal welfare of the Kanton Bern, Switzerland (permission number 76/07 for EAE and 116/07 for IVM). Wild-type SJL/J mice were obtained from Harlan (Horst, Netherlands) for the first series of experiments and because of discontinuation of this colony from Harlan UK (Bicester, Oxon, U.K.) for the remaining series of experiments. Wild-type C57BL/6 mice were purchased from Harlan UK. C57BL/6 mice carrying two floxed β_1 integrin alleles were intercrossed with C57BL/6 mice carrying an Mx1 promoter-driven Cre recombinase transgene and kept on the C57BL/6 genetic background (16).

EAE induction

Female SJL/J mice (7–10 wk old) were immunized s.c. with 50 μg proteolipid protein peptide ($PLP_{aa\ 139–151}$) in CFA (Santa Cruz; LabForce, Nunningen, Switzerland) supplemented with 4 mg/ml nonviable, desiccated *Mycobacterium tuberculosis* (H37RA; Difco Laboratories, Detroit, MI) exactly as described previously (17). A total of 300 ng

pertussis toxin from *Bordetella pertussis* (LuBioScience, Lucerne, Switzerland) permouse were administered i.p. at days 1 and 3 postimmunization. In agreement with the local government, assessment of clinical disease activity was performed twice daily as described before (18) using a four-point scoring system as follows: 0, healthy; 0.5, limp tail; 1, hind leg paraparesis; 2, hind leg paraplegia; and 3, hind leg paraplegia with incontinence. For reasons of standardization for IVM experiments, we specifically used animals at days 10 and 11 postimmunization with a disease score of 0.5 or 1. We did not observe any difference in EAE development in SJL/J mice obtained from the Harlan colonies in the Netherlands or the United Kingdom.

Monoclonal Abs

Rat anti-mouse α_4 integrin (PS/2), rat anti-mouse $\alpha_4\beta_7$ integrin (DATK-32), and rat anti-mouse β_7 integrin (Fib 504) for in vivo use were purified from serum-free hybridoma culture supernatants. Endotoxin level, determined using Endosafe test (Charles River Laboratories, Sulzfeld, Germany), was below detection level. Endotoxin-free rat IgG2b was used as isotype control. The rat anti-mouse mAbs used for FACS analysis in this study were serum-free culture supernatants of hybridoma cells: PS/2 (rat anti-mouse α_4 integrin IgG2b), 9B5 (rat anti-human CD44 IgG2a), DATK-32 (rat anti-mouse $\alpha_4\beta_7$ integrin IgG2a), Fib504 (rat anti-mouse β_7 integrin IgG2a), FD441.8 (rat anti-mouse CD11a IgG2b), MEC 13.3 (rat anti-mouse CD31 IgG2a), M1/70 (rat anti-mouse CD11b IgG2b), 4RA.10 (rat anti-mouse PSGL-1 IgG1), Kat.1 (rat anti-mouse ICAM-1 IgG2a), and KM201 (rat anti-mouse CD44 IgG1). PE–anti-CD29 (β_1 integrin, clone HMβ1-1) mAb and PE-Armenian hamster IgG isotype control (clone HTK888) were purchased from BioLegend (San Diego, CA), and PE-CD11c (clone N418) was purchased from eBioscience (Frankfurt/Main, Germany). Rat anti-mouse CD86 (clone GL-1) was obtained from Pharmingen BD Biosciences (Basel, Switzerland), and rat anti-mouse CD205 was obtained from AbD Serotec (Düsseldorf, Germany). Rat anti-mouse MHC class II (ER-TR2, rat IgG2b) was purchased from BMA Biomedicals (Augst, Switzerland). PE-conjugated $F(ab')_2$ goat anti-rat Ig (BioSource International, Camarillo, CA) was used as secondary Ab.

Flow cytometry

For the FACS analysis 0.5×10^6 cells/sample were washed twice with FACS buffer (PBS supplemented with 2.5% FBS and 0.1% NaN_3) and incubated either with culture supernatant containing mAb specific for each cell surface molecule or purified commercial mAbs at 10 μg/ml FACS buffer. After 30 min of incubation on ice, cells were washed twice with FACS buffer. Cells were then incubated with PE-conjugated secondary Ab in FACS buffer/10% normal mouse serum for 30 min on ice. After washing twice, cells were fixed in 1% formaldehyde/PBS (pH 7.4). Flow cytometry analysis was performed on a FACSCalibur using CellQuest software (BD Biosciences, Heidelberg, Germany).

Dendritic cells

Mouse BM-derived DCs were prepared as previously described (19) with some minor modifications. Briefly, 2×10^6/ml BM cells were cultured in RPMI 1640 medium supplemented with 10% FBS, 2-mM L-glutamine,1mM sodium pyruvate, 100 U penicillin-

streptomycin, 0.05 mM 2-ME, and 20% of Flt-3L–containing supernatant [produced from SP2/0 transfectants secreting mouse recombinant Flt-3L (20)]. Where indicated, DCs were matured with 1 μg/ml LPS (Sigma-Aldrich, Buchs, Switzerland) during the last 20 h of culture. After 8–10 d, nonadherent and loosely adherent cells were collected, and dead cells were removed using a Dead Cell Removal Kit (Miltenyi Biotec, Bergisch Gladbach, Germany). DCs were labeled with 2.5 μM Cell Tracker Green (5-chloromethylfluorescein diacetate, CMFDA; Molecular Probes, Eugene, OR) and then subjected to a Nycoprep 1.077A gradient (Axis-Shield PoC, Oslo, Norway) revealing a DC viability of 100% and DC purity of >90% based on FACS analysis for CD11c. To obtain BM-derived β_1 integrin-deficient DCs and respective control DCs, mice carrying a floxed β_1 integrin gene (C57BL/6–*Itgb2tm/Ref*) were intercrossed with mice carrying an Mx1 promoter-driven Cre recombinase transgene [C57BL/6–*Tg(Mx1.-cre)1Cgn*] (16). $\beta1^{fl/fl}$/MxCre^{+} mice and $\beta1^{fl/fl}$/MxCre^{-} mice received a single i.p. injection of 250 μg polyIC polyriboinosinic-polyribocytidylic acid (GE Healthcare, Otelfingen, Switzerland) in PBS 12 d prior to cell isolation. BM-derived DCs were prepared as described above. Depletion of β_1 integrin on the DCs was confirmed by FACS analysis. We did not observe any differences in amount and purity of Flt-3L–differentiated DCs isolated from the BM of SJL/J or C57BL/6 mice.

Surgical preparation of the spinal cord window

The surgical preparations and experiments were performed in accordance with the Swiss legislation. The spinal cord window preparation was carried out exactly as described previously (15, 21). Briefly, mice were anesthetized by s.c. injection of ketamin/xylazine, and the right common carotid artery was catheterized for injection of fluorescently labeled cells and tetramethylrhodamine isothiocyanate (TRITC)-dextran as a plasma marker. Next, the animal was turned to the prone position, and the head was fixed in a stereotactic rodent head holder. A laminectomy was conducted from C2 to C7 under microscopic control. The dura above that area was removed. To prevent the tissue from dehydration, the preparation was covered with an impermeable transparent membrane. Only preparations showing no bleeding and intact microcirculation were considered acceptable for subsequent examination by intravital microscopy.

Intravital epifluorescence videomicroscopy

For IVM, the animals were transferred to the microscope stage remaining within the stereotactic head holder. Normal body temperature was maintained throughout the entire experiment. IVM was performed by epi-illumination techniques using a Mikron IVM500 microscope (Mikron Instruments, San Marcos, CA) coupled with a 50-W mercury lamp (HBO 50 microscope illuminator; Zeiss, Feldbach, Switzerland) and combined with blue (exciter 455DF70, dichroic 515DRLP, and emitter 515ALP) and green (exciter 525DF45, dichroic 560DRLP, and emitter 565ALP) filter blocks. Observations were made using ×4, ×10, and ×20 long-distance working objectives (Zeiss). All experiments were recorded by means of a low-light level silicone intensified target-video camera with an optional image intensifier for weak fluorescence (DAGE-MTI, Michigan City, IN). The data were transferred to a digital video system for later off-line analysis of DC interaction within the CNS micro-vessels. Prior to cell infusion, 1% TRITC-conjugated dextran/0.9% NaCl was injected to visualize the spinal cord microvasculature. DCs were incubated either with an

isotype control rat IgG2b mAb or with rat anti-mouse α_4 integrin IgG2b mAb (PS/2) or with rat anti-mouse β_7 integrin IgG2b mAb (Fib504) at 105 μg Ab/3.5 × 10^6 cells in 300 μl 0.9% NaCl or with rat anti-mouse $\alpha_4\beta_7$ integrin IgG2b mAb DATK32 at 210 μg Ab/3.5 × 10^6 cells in 300 μl 0.9% NaCl for precisely 20 min at 37°C to ensure the appropriate infusion temperature of the DCs. Cells were systemically injected in three subsequent identical aliquots via the right common carotid artery leading to the direct transport of cells into the area of interest, where interactions were observed and recorded in real time in three independent sequences as described before (15, 16, 21, 22).

Intravital microscopic image analysis

Hemodynamic parameters—The hemodynamic parameters of the blood flow were evaluated for each analyzed postcapillary venule as follows: the mean blood flow velocity (V_{blood}) represents $V_{blood} = V_{max}/2 - [D_L/D_V]^2$ (μm/s), where V_{max} is the velocity of the fastest noninteracting DCs. D_L represents the DC diameter and D_V the vessel diameter (23, 24). To quantify the force acting on rolling or adherent leukocytes, the wall shear rate (γ) was evaluated for each venule as $\gamma = V_{blood} \times 8/D_V$ (s^{-1}). The wall shear stress (τ), dependent on blood viscosity (assumed to be 0.0025 poise), was calculated as $\tau = \gamma \times 0.0025$ (dyne/cm^2) (24). We did not observe any significant difference in hemodynamic parameters between groups of SJL mice with EAE infused with either immature DCs isolated from SJL/J or C57BL/6 mice.

Off-line analysis of DC-endothelial interactions—DCs passing through spinal cord microvessels and DCs, which visibly initiated contact with the spinal cord microvascular endothelium and thus moved at a slower velocity than circulating DCs, were counted during the three observation periods of 1 min each in frame-by-frame analysis of the videos using the CapImage software (version 8.3; Dr. H. Zeintl Biomedical Engineering, Heidelberg, Germany). The fraction of DCs initiating contact with the vascular wall was calculated for each microvessel as the percentage of interacting DCs among the total number of DCs passing through a given postcapillary venule during these 1-min observation windows. The rolling fractions and the capture fractions were counted accordingly. Permanently adherent DCs were identified as cells stuck to the vessel wall without moving or detaching from the endothelium for a period of ≥20 s and were counted 10 min, 30 min, and 1 h postinjection. The observer was unbiased and blinded for the experiments and analyses performed. We did not observe any difference in the capacity of immature DCs from C57BL/6 mice to initiate contact by either rolling or capturing and to firmly adhere to the inflamed BBB endothelium in SJL mice with EAE compared with immature DCs isolated from SJL/J mice.

Immunofluorescence and quantification of DCs

Three to 4 h after DC infusion, anesthetized mice were perfused with 1% paraformaldehyde/PBS. Spinal cords were embedded in OCT compound and frozen (Sakura Finetek, Alphen aan den Rijn, The Netherlands). Longitudinal sections were cut at 6 μm on a cryostat. Slides were fixed 10 min with ice-cold acetone and dried. Following rinsing with 0.1 M TBS, slides were incubated for 20 min with TBS containing 5% skimmed milk and 0.3% Triton X-100. After washing with 0.1 M TBS, slides were incubated for 1 h with a polyclonal rabbit anti-laminin Ab (1/4000; DakoCytomation, Glostrup, Denmark) to define both

basement membranes and outline the leptomeninges. After washing with 0.1 M TBS, slides were incubated with a secondary Ab 7-amino-4-methylcoumarin-3-acetic acid–conjugated $F(ab')_2$ fragment goat anti-rabbit IgG (1/100; Jackson ImmunoResearch Laboratories, West Grove, PA) for 1 h. Negative controls used appropriate species-specific, nonimmune IgG to nullify any background staining. The total number and distribution of immature DCs was counted in three longitudinal spinal cord sections per mouse along the dorsal-ventral axis of the spinal cord. In relation to the laminin, stained DCs were assigned to the following compartments: meningeal space, intravascular, perivascular, and parenchymal.

Statistical analysis

All statistical analysis was performed using the GraphPad Prism software (version 5.00; GraphPad, San Diego, CA). Data are presented as medians with interquartile ranges. Mann-Whitney *U* statistics were used for comparisons between different data sets. Asterisks indicate significant differences (*$p < 0.05$; **$p < 0.01$; ***$p < 0.005$). For analysis of adherent DCs in the IVM analysis, mean values were calculated from the values in each animal, and the two groups were compared using a Mann-Whitney *U* test.

Results

Phenotype of Flt-3L–differentiated DCs

To investigate the multistep DC-endothelial interactions involved in the recruitment of DC into the CNS in vivo, we generated Flt-3L–differentiated DCs from mouse BM precursors in vitro (19). After 8–10 d in culture, the cell surface phenotype of Flt-3L–differentiated DCs was assessed by flow cytometry (Fig. 1). Purity of the DC populations was shown to be >90% based on immunostaining for CD11c (Fig. 1*A*). No expression of the MHC class II, CD86, and CD205 was detected, confirming the immature state of Flt-3L–differentiated DCs. We also did not observe any significant differences in the phenotype of DCs isolated from SJL/J and C57BL/6 mice. Maturation of Flt-3L–differentiated DCs was induced by overnight stimulation with 1 μg/ml LPS. LPS-matured DCs displayed upregulated expression of MHC class II, CD86, and CD205 and CD54 (Fig. 1*B*) as reported previously (25). Interestingly, immature and LPS-matured DCs did—with the exception to α_4 integrins—not show any significant differences in their expression of cell surface adhesion molecules potentially involved in trafficking to the CNS (Fig. 1*C*).

Initiation of interaction of immature versus LPS-matured Flt-3L–differentiated DCs with the inflamed BBB during EAE

We next investigated the ability of immature and LPS-matured DCs to interact with the inflamed spinal cord white-matter microvasculature in SJL mice afflicted with $PLP_{aa\ 139–151}$-induced EAE by IVM through a spinal cord window preparation. As described by us before, this technique allows the direct visualization of potential interactions of circulating immune cells with the CNS micro-vessels under pathophysiological shear forces in vivo (15, 16, 22). After contrast enhancement of the microcirculation by injection of TRITC-dextran, 3.5×10^6 fluorescently labeled immature DCs were systemically infused in three individual injections via the right common carotid artery. Immature DCs could readily be observed to pass through the spinal cord white-matter microvessels and to initiate

contact with the inflamed CNS endothelium (Fig. 2*A*, black bars, Supplemental Movie 1). Contact initiation was mediated either by rolling of the immature DCs, characterized by their movement with reduced velocity along the vascular wall, or to a lesser degree by capturing, that is, an abrupt stop of the DCs on the vascular wall. Interestingly, LPS-matured DCs showed a similar capacity to engage in rolling and capturing on the inflamed spinal cord BBB when compared with immature DCs (Fig. 2*A*, gray bars, Supplemental Movie 2).

Adhesion of immature versus LPS-matured Flt-3L–differentiated DCs to the inflamed BBB during EAE

Next, we asked whether the initial interaction of immature versus mature DCs with the inflamed BBB would translate into their firm adhesion to the BBB. We therefore quantified the number of DCs permanently adhering within the inflamed spinal cord microvessels at different time points (10 min, 30 min, and 1 h) after DC infusion for both immature DCs (Fig. 2*C*, 2*E*, Supplemental Movie 3) and LPS-matured DCs (Fig. 2*D*, 2*E*, Supplemental Movie 4). Immature and also LPS-matured DCs were found to undergo firm and sustained adhesion to the inflamed BBB endothelium in vivo. Surprisingly, the numbers of immature DCs found to firmly adhere to the inflamed spinal cord BBB were ~5-fold higher as compared with the numbers of LPS-matured DCs found to remain adherent to the inflamed spinal cord microvascular wall during EAE ($p < 0.0001$ at 10 min). Thus, although immature and LPS-matured DCs engage with the same efficiency into the first step of the multistep interaction with the inflamed BBB, immature DCs show a dramatically enhanced ability to firmly adhere to the BBB endothelium in vivo when compared with LPS-matured DCs.

Hemodynamic parameters in spinal cord microvessels during EAE

To exclude that the different efficiency of immature versus LPS-matured DCs to firmly adhere to the inflamed BBB in vivo depends on differences in hemodynamic parameters between the two experimental groups, the mean microvessel diameter, mean DC velocity, wall shear stress, and wall shear rates were determined. None of these hemodynamic parameters displayed a significant difference between the mice infused with immature versus those infused with LPS-matured DCs (Fig. 3). Thus, hemodynamic parameters did not account for the different efficiency of immature versus LPS-matured DCs to roll on or capture to the inflamed BBB during EAE in vivo.

Migration of immature versus LPS-matured Flt-3L–differentiated DCs across the inflamed BBB during EAE

To finally address whether immature DCs compared with LPS-matured DCs have a higher efficiency in extravasating across the BBB, we performed immunofluorescence studies of serial frozen sections of spinal cords from mice infused with fluorescently labeled DCs 3 or 4 h prior to tissue preparation. Counterstaining for laminin was used to visualize the endothelial and parenchymal basement membranes of the CNS microvessels. At 3 and 4 h after infusion, immature DCs could still be observed within the lumen of spinal cord white-matter microvessels but were also detected on their way across the endothelial cell wall, within the perivascular spaces, and beyond the parenchymal basement membrane of CNS microvessels, demonstrating that immature DCs readily penetrate inflamed spinal cord

white-matter microvessels (Fig. 4*A*, 4*B*, 4*D*). The highest number of immature DCs was, however, found to infiltrate the meningeal compartment, where they could be detected outside of the vasculature (Fig. 4*C*, 4*D*). In contrast, only individual LPS-matured DCs could be detected in the spinal cord frozen tissue sections 3 and 4 h after DC infusion. In this case, all LPS-matured DCs were still found within the lumen of the spinal cord white-matter microvessels (Fig. 4*E*), suggesting that LPS-matured DCs cannot cross the parenchymal BBB to enter the spinal cord white-matter parenchyma. In contrast, LPS-matured DCs could migrate across meningeal microvessels, because we could detect them outside of blood vessels within the meningeal compartment (Fig. 4*F*).

α_4 Integrins mediate adhesion but not rolling and capturing of Flt-3L–differentiated DCs on the inflamed BBB during EAE

We finally aimed to determine the molecular mechanisms mediating DC interaction with the inflamed BBB during EAE. The obvious adhesion molecules to investigate in this context were the α_4 integrins, because blocking α_4 integrins were shown to inhibit T cell recruitment into the CNS and the development of clinical EAE (14). Involvement of α_4 integrins in the recruitment of immune cells other than T cells across the inflamed BBB during EAE has not been addressed in detail. We found both α_4 integrins, $\alpha_4\beta_1$ and $\alpha_4\beta_7$, to be present on the cell surface of immature and LPS-matured DCs (Fig. 1*C*). Therefore, we asked whether blocking α_4 integrins on the DC surface would influence their interaction with the inflamed BBB during EAE. Pretreatment of immature or LPS-matured DCs with a blocking anti-α_4 integrin mAb had no effect on their intrinsic abilities to initiate contact with the inflamed spinal cord BBB (Fig. 2*B*, open circles) and also did not influence hemodynamic parameters (Fig. 3) when compared with rat IgG2b control-treated DCs (Figs. 2*B*, closed circles, 3). A lack of involvement of α_4 integrins in mediating the initial interaction of DCs with the spinal cord microvasculature was confirmed by the observation that blocking of α_4 integrins failed to change rolling velocities of DCs when compared with rat IgG2b control-treated DCs (Supplemental Fig. 1). In contrast, blocking α_4 integrins significantly reduced the firm adhesion of immature DCs (Fig. 2*C*, 2*E*) and LPS-matured DCs (Fig. 2*D*, 2*E*) to the spinal cord microvasculature when compared with IgG2b isotype control treatment, respectively, as already observed 10 min after DC infusion (Fig. 2*C*, 2*D*). The reduced adhesion of immature and LPS-matured DCs pretreated with anti-α_4 integrin mAb to the inflamed BBB was sustained over time, as numbers of DCs found to adhere to the spinal cord microvasculature remained low at 30 min and 1 h after DC injection (Fig. 2*C*, 2*D*). It should be noted in this paper that differences were observed in the amount of inhibition exerted by the anti-α_4 integrin Ab treatment on DC adhesion between early (85% inhibition) and later (50% inhibition) experiments performed in SJL/J mice from different colonies of the provider. Although we did not observe any overt difference in EAE development or any significant difference in the hemodynamic parameters within the spinal cord microcirculation during EAE, we speculate this to be because of subtle differences in CNS inflammation established in SJL/J mice obtained from two different colonies.

Immunofluorescence studies of serial frozen sections of spinal cords from mice infused with fluorescently labeled anti-α_4 integrin mAb pretreated immature or LPS-matured DCs 3 or 4

h before tissue preparation either failed to detect any DC outside of inflamed CNS microvessels or yielded a negligible number of cells (data not shown).

Thus, α_4 integrins specifically mediate the firm adhesion of DCs—irrespective of their maturation stage—to the inflamed BBB and thus are required for successful migration of DCs across the BBB during EAE.

β_7 Integrins are not required for rolling, capturing and adhesion of Flt-3L–differentiated DCs on the inflamed BBB during EAE

We next aimed to determine which α_4 integrin—$\alpha_4\beta_1$ or $\alpha_4\beta_7$ integrin—mediates the firm adhesion of immature DCs to the inflamed BBB. To this end, we first addressed whether pre-treatment of immature DCs with a blocking anti-β_7 integrin mAb would influence their interaction with the inflamed spinal cord white-matter microvasculature in SJL mice with EAE. We observed that blocking β_7 integrins on immature DCs did not affect their ability to initiate contact with the inflamed spinal cord microvascular wall (Fig. 2*B*, light gray filled circles) when compared with isotype control- or anti-α_4 integrin Ab-treated immature DCs (Fig. 2*B*). In contrast to blocking α_4 integrins, blocking of β_7 integrins on immature DCs, however, failed to interfere with their ability to firmly adhere to the inflamed spinal cord microvasculature. We did not observe any reduction in the number of anti-β_7 integrin mAb-pretreated immature DCs firmly adhering to the inflamed BBB when compared with isotype control conditions at 10 min, 30 min, and 1 h after DC infusion. Finally, blocking β_7 integrins also had no effect on DC entry into the CNS, which was found to occur to the same degree as under control conditions (Fig. 4 and data not shown). Because the hemodynamic parameters in those mice infused with anti-β_7 integrin-pretreated DCs also did not differ from the isotype control treatment or the anti-α_4 integrin mAb treatment group (Fig. 3), our results clearly demonstrate that β_7 integrins are not required for the recruitment of DCs across the inflamed BBB in EAE.

$\alpha_4\beta_1$ Integrin mediates the adhesion of Flt-3L–differentiated immature DCs to the inflamed BBB during EAE

Lack of requirement of β_7 integrins for the interaction of immature DCs with the inflamed BBB during EAE suggested that $\alpha_4\beta_1$ integrin is responsible for mediating the firm adhesion of immature DCs to the inflamed spinal cord microvasculature. To test this, we generated β_1 integrin$^{-/-}$ immature DCs from $\beta1^{fl/fl}$/MxCre^{+} C57BL/6 mice (16). Purity of $\beta1^{-/-}$ immature DCs was >90% as shown by immunostaining for CD11c and therefore identical to the purity of immature DCs isolated from SJL/J and C57BL/6 mice (Fig. 1*A*) (data not shown). Cre-mediated deletion of the β_1 integrin subunit in immature DCs was found to be complete as shown by the lack of immunostaining for the β_1 integrin subunit (Fig. 1*D*). As already observed for β_1 integrin$^{-/-}$ T cells (16, 26), β_1 integrin$^{-/-}$ DCs were, however, found to express higher cell surface levels of the β_7 subunit and $\alpha_4\beta_7$ integrin when compared with control immature DCs from SJL/J and C57BL/6 mice (Fig. 1*A*, 1*D*) (data not shown).

We first addressed the ability of β_1 integrin$^{-/-}$ DCs to initiate contact with the spinal cord microvascular endothelium in EAE when compared with DCs treated with IgG2b isotype

control mAb or with a blocking anti-$\alpha_4\beta_7$ integrin mAb (DATK32). Although β_1 integrin$^{-/-}$ DCs were found to show a reduced capacity to capture to the spinal cord microvascular wall when compared with control DCs, their ability to initiate contact with the inflamed BBB by rolling along the vessel wall was not impaired (Fig. 5*A*). Because the percentage of DCs initiating their interaction with the inflamed spinal cord microvasculature by rolling is much higher than that of DCs initiating interaction by capturing, taken together, the initial contact fraction of β_1 integrin$^{-/-}$ DCs was found to be indistinguishable from that of control DCs (Fig. 5*A*). In accordance to our findings that neither blocking of α_4 nor of β_7 integrins inhibits the initial contact of DCs to the spinal cord microvascular wall, blocking of $\alpha_4\beta_7$ integrin was also found to have no impact on DC-mediated rolling or capturing on the spinal cord microvasculature in vivo (Fig. 5*A*). Furthermore, infusion of β_1 integrin$^{-/-}$ immature DCs or of anti-$\alpha_4\beta_7$ integrin mAb-preincubated DCs did not cause alterations of hemodynamic parameters in the spinal cord microvasculature of SJL mice with EAE (Fig. 3).

Investigating the role of $\alpha_4\beta_7$ integrin in mediating the firm adhesion of immature DCs to the microvascular wall of the spinal cord, we found no difference in the number of anti-$\alpha_4\beta_7$ integrin mAb-pretretated DCs firmly adhering to the inflamed BBB at 10 min, 30 min, and 1 h after infusion when compared with the IgG2b isotype control (Fig. 5*B*, 5*C*). In contrast, β_1 integrin$^{-/-}$ DCs exhibited a significantly reduced firm adhesion to the spinal cord microvasculature when compared with either IgG2b isotype control or anti-$\alpha_4\beta_7$ integrin Ab treatment (Fig. 5*B*, 5*C*). This significantly reduced adhesion of β_1 integrin$^{-/-}$ immature DCs observed 10 min after cell infusion was sustained at 30 min and 1 h and was comparable to the reduced adhesion of immature DCs observed in the functional absence of α_4 integrins in this set of experiments as explained above. Taken together, these data demonstrate that $\alpha_4\beta_1$ but not $\alpha_4\beta_7$ integrin mediates the firm adhesion of immature DCS to the inflamed spinal cord microvasculature during EAE.

Discussion

DCs have come to be recognized as important regulators of CNS autoimmune inflammatory responses. During MS and its animal model EAE, accumulation of DCs is readily observed within inflammatory infiltrates in the CNS parenchyma (2, 3, 6, 7) and additionally in the cerebrospinal fluid of MS patients (5), suggesting that DCs might play a key role in determining the outcome of CNS inflammation. The important role of DCs in EAE pathogenesis is underlined by the observations that CD11c$^{-/-}$ mice are resistant to EAE (27) and that CD11c^{+} DCs are sufficient to present Ag to primed myelin-reactive T cells in vivo to mediate CNS inflammation and clinical EAE (2). In addition, DCs have been implicated in epitope spreading during chronic EAE (9) and have been shown to be particularly well suited to polarize myelin-specific T cells toward Th1 and Th17 effector T cells in vitro (8, 28). In fact, very recently, intracerebral DCs have even been shown to modulate encephalitogenic versus regulatory immune responses in the CNS (10).

Although it has thus been well established that DCs are pivotal players in the development of CNS autoimmune inflammation, the molecular mechanisms of how circulating DCs gain access to the CNS have not been investigated in vivo. Most studies have focused on

investigating the multistep recruitment of encephalitogenic T cells across the BBB during EAE (summarized in Ref. 29). Recently, we showed that T cells but not myeloid cells critically depend on β_1 integrins to enter the CNS during EAE (16), suggesting that during EAE DCs may use molecular mechanisms to enter the CNS that are distinct from those used by T cells.

In this paper, we have specifically addressed the trafficking of circulating DCs across the BBB during EAE by means of IVM (15, 16).

Direct visualization of the inflamed mouse spinal cord white-matter microcirculation in mice with EAE allowed us to observe the rolling, capture, and firm adhesion of infused fluorescently labeled DCs within this vascular bed in vivo. Immature and LPS-matured BM-derived DCs effectively initiated contact with the BBB endothelium by rolling and capturing, then firmly adhered to the inflamed mouse spinal cord white-matter microvasculature and finally extravasated across the BBB into the CNS. Our observations are in line with previous studies observing that immature but not mature BM-derived DCs accumulated in inflamed ear skin after i.v. injection (30, 31). Besides focusing on the anatomical localization of immature versus LPS-matured DCs in relation to CNS blood vessels, we aimed to quantify extravasation of immature versus LPS-matured DCs into the CNS and found a pronounced difference in the ability of immature versus mature DCs to extravasate across the inflamed BBB in the spinal cord white matter during EAE. Whereas LPS-matured DCs were restricted to extravasate across the meningeal BBB, immature DCs were able to cross the BBB of the spinal cord parenchyma over a time course of 4 h. Nevertheless, also immature DCs were found to preferentially extravasate across meningeal blood vessels. Our observations therefore confirm the notion that the migratory ability of DCs is intrinsically linked to their maturation state and that differences in traffic signals displayed on the surface of immature versus mature DCs might influence their efficiency to enter certain inflammatory sites (32). Furthermore, there are subtle differences between the BBB characteristics of meningeal and parenchymal microvessels (33). Thus, the properties of BBB endothelial cells that determine DC extravasation into the CNS may be different in the meningeal space as compared with the CNS parenchyma (34). The former but not the latter lack astrocytic ensheathment, whereas the latter are deficient for P-selectin storage (35). Thus, meningeal and parenchymal BBB endothelium might provide different molecular traffic cues for circulating DCs, allowing the penetration of mature DCs solely across the meningeal BBB. LPS-matured DCs are known to have reprogrammed their repertoire of adhesion and chemokine receptors specifically to migrate to lymph nodes (32). Despite the lack of classical lymphatic vessels in the CNS, soluble CNS Ags and probably also APCs do reach the CNS-draining lymph nodes (36). Drainage of the CNS occurs via the cerebrospinal fluid, which is also filling the meningeal compartment. Thus, extravasation of LPS-matured DCs into the meningeal compartment may reflect their natural pathway of CNS immuno-surveillance via the meningeal space and subsequent migration to the local draining lymph nodes.

To determine the molecular mechanisms of DC entry to the CNS, we next asked which adhesion receptors may be involved in DC/BBB interactions during EAE. Following the seminal study by Yednock et al. (37), numerous studies have confirmed that blocking α_4

integrins inhibits inflammatory cell recruitment into the CNS and the development of clinical EAE (14). These findings have been translated into a novel therapy of MS with the humanized anti-α_4 integrin Ab natalizumab. T cells have been shown to be the target of the anti-α_4 integrin therapy because they critically depend on $\alpha_4\beta_1$ integrins to capture and adhere to the healthy BBB (15) and to firmly adhere to the inflamed BBB during EAE (16). Involvement of α_4 integrins in the recruitment of immune cells other than T cells across the inflamed BBB during EAE has not been addressed in any detail. Our study demonstrates that firm adhesion, but not rolling and capturing, of both immature and LPS-matured DCs to the BBB was mediated by α_4 integrins. By specifically comparing the interaction of immature DCs with the inflamed BBB during EAE in the functional absence of α_4 integrins, β_7 integrins, β_1 integrins, and $\alpha_4\beta_7$ integrin, we found that firm adhesion, but not rolling and capturing, of immature DCs to the BBB was mediated by $\alpha_4\beta_1$ integrin. To the best of our knowledge, our study represents the first live imaging study on DC trafficking across the BBB that demonstrates an involvement of $\alpha_4\beta_1$ integrin in this process.

Therefore, in addition to T cells therapeutic targeting of α_4 integrins in EAE and MS may also affect the trafficking of DCs across the BBB and thus resolve CNS autoimmune inflammation by depleting the CNS of professional APCs. In light of the recent observation that encephalitogenic T cells may first extravasate across meningeal vessels and then need to encounter their specific Ag in the subarachnoid space before entering the CNS parenchyma and triggering clinical EAE (38), the preferential extravasation of immature and mature DCs across meningeal vessels observed in our study is of interest. Depleting the subarachnoid space of DCs may lead to insufficient activation of autoagressive T cells in this compartment, resulting in a failure to develop the effector functions required to induce or maintain clinical EAE. Finally, this notion is supported by the recent finding that in cerebral autopsy material of a patient with MS who developed progressive multifocal leukoencephalopathy during natalizumab therapy, the expression of MHC class II molecules and the number of $CD209^+$ DCs were found to be significantly decreased in cerebral perivascular spaces when compared with location-matched cerebral autopsy material of patients without CNS disease, MS patients not treated with natalizumab, or patients with progressive multifocal leukoencephalopathy not associated with natalizumab therapy (39).

Taken together, our present study provides direct evidence for the ability of circulating DCs to migrate across the inflamed BBB during EAE. The maturation status of the DCs influences their ability to enter different CNS compartments. Whereas immature DCs can cross the inflamed BBB in the CNS white-matter parenchyma and the meningeal compartment, mature DCs were found to be solely able to enter the meningeal space. In their respective CNS locations, DCs may contribute to the perpetuation of the CNS autoimmune attack by continuous Ag presentation and epitope spreading. On the basis of our present findings that both immature and mature DCs depend on α_4 integrins to firmly adhere to the inflamed BBB, we propose that therapeutic targeting of α_4 integrins in EAE and MS may besides inhibiting T cell entry into the CNS block the recruitment of circulating DCs into the CNS and therefore stop activation of autoantigen-specific $CD4^+$ T cells within the CNS. Depletion of DCs inside the CNS by targeting α_4 integrins could explain the long-lasting therapeutic effects of natalizumab shown to produce reduced T lymphocyte counts in the cerebrospinal fluid of MS patients even 6 mo after cessation of natalizumab treatment (40).

Supplementary Material

Refer to Web version on PubMed Central for supplementary material.

Acknowledgments

We thank Heidi Tardent for excellent microsurgical preparations. We also thank Reinhard Fässler for providing the $\beta1^{fl/fl}/MxCre^{+}$ mice and for the gift of polyIC.

This work was supported by the National Multiple Sclerosis Society and the Swiss Multiple Sclerosis Society (to B.E.), by a Professional Enrichment and Growth grant from the Drexel University College of Medicine (to P.J.), and by the National Multiple Sclerosis Society (to C.C.).

Abbreviations used in this paper

BBB	blood-brain barrier
BM	bone marrow
DC	dendritic cell
EAE	experimental autoimmune encephalomyelitis
FOV	field of view
IVM	intravital fluorescence videomicroscopy
MS	multiple sclerosis
TRITC	tetramethylrhodamine isothiocyanate

References

1. Matyszak MK, Perry VH. The potential role of dendritic cells in immune-mediated inflammatory diseases in the central nervous system. Neuroscience. 1996; 74:599–608. [PubMed: 8865208]
2. Greter M, Heppner FL, Lemos MP, Odermatt BM, Goebels N, Laufer T, Noelle RJ, Becher B. Dendritic cells permit immune invasion of the CNS in an animal model of multiple sclerosis. Nat. Med. 2005; 11:328–334. [PubMed: 15735653]
3. McMahon EJ, Bailey SL, Castenada CV, Waldner H, Miller SD. Epitope spreading initiates in the CNS in two mouse models of multiple sclerosis. Nat. Med. 2005; 11:335–339. [PubMed: 15735651]
4. Fabriek BO, Van Haastert ES, Galea I, Polfliet MM, Döpp ED, Van Den Heuvel MM, Van Den Berg TK, De Groot CJ, Van Der Valk P, Dijkstra CD. CD163-positive perivascular macrophages in the human CNS express molecules for antigen recognition and presentation. Glia. 2005; 51:297–305. [PubMed: 15846794]
5. Pashenkov M, Huang YM, Kostulas V, Haglund M, Söderström M, Link H. Two subsets of dendritic cells are present in human cerebrospinal fluid. Brain. 2001; 124:480–492. [PubMed: 11222448]
6. Serafini B, Rosicarelli B, Magliozzi R, Stigliano E, Capello E, Mancardi GL, Aloisi F. Dendritic cells in multiple sclerosis lesions: maturation stage, myelin uptake, and interaction with proliferating T cells. J. Neuropathol. Exp. Neurol. 2006; 65:124–141. [PubMed: 16462204]
7. Serafini B, Columba-Cabezas S, Di Rosa F, Aloisi F. Intracerebral recruitment and maturation of dendritic cells in the onset and progression of experimental autoimmune encephalomyelitis. Am. J. Pathol. 2000; 157:1991–2002. [PubMed: 11106572]
8. Deshpande P, King IL, Segal BM. Cutting edge: CNS $CD11c^{+}$ cells from mice with encephalomyelitis polarize Th17 cells and support $CD25^{+}$ $CD4^{+}$ T cell-mediated

immunosuppression, suggesting dual roles in the disease process. J. Immunol. 2007; 178:6695–6699. [PubMed: 17513712]

9. Miller SD, McMahon EJ, Schreiner B, Bailey SL. Antigen presentation in the CNS by myeloid dendritic cells drives progression of relapsing experimental autoimmune encephalomyelitis. Ann. N. Y. Acad. Sci. 2007; 1103:179–191. [PubMed: 17376826]
10. Zozulya AL, Ortler S, Lee J, Weidenfeller C, Sandor M, Wiendl H, Fabry Z. Intracerebral dendritic cells critically modulate encephalitogenic versus regulatory immune responses in the CNS. J. Neurosci. 2009; 29:140–152. [PubMed: 19129392]
11. Ifergan I, Kébir H, Bernard M, Wosik K, Dodelet-Devillers A, Cayrol R, Arbour N, Prat A. The blood-brain barrier induces differentiation of migrating monocytes into Th17-polarizing dendritic cells. Brain. 2008; 131:785–799. [PubMed: 18156156]
12. King IL, Dickendesher TL, Segal BM. Circulating Ly-6C$^+$ myeloid precursors migrate to the CNS and play a pathogenic role during autoimmune demyelinating disease. Blood. 2009; 113:3190–3197. [PubMed: 19196868]
13. Zozulya AL, Reinke E, Baiu DC, Karman J, Sandor M, Fabry Z. Dendritic cell transmigration through brain microvessel endothelium is regulated by MIP-1α chemokine and matrix metalloproteinases. J. Immunol. 2007; 178:520–529. [PubMed: 17182592]
14. Engelhardt B. Regulation of immune cell entry into the central nervous system. Results Probl. Cell Differ. 2006; 43:259–280. [PubMed: 17068976]
15. Vajkoczy P, Laschinger M, Engelhardt B. α_4 Integrin-VCAM-1 binding mediates G protein-independent capture of encephalitogenic T cell blasts to CNS white matter microvessels. J. Clin. Invest. 2001; 108:557–565. [PubMed: 11518729]
16. Bauer M, Brakebusch C, Coisne C, Sixt M, Wekerle H, Engelhardt B, Fässler R. β_1 Integrins differentially control extravasation of inflammatory cell subsets into the CNS during autoimmunity. Proc. Natl. Acad. Sci. USA. 2009; 106:1920–1925. [PubMed: 19179279]
17. Döring A, Wild M, Vestweber D, Deutsch U, Engelhardt B. E-and P-selectin are not required for the development of experimental autoimmune encephalomyelitis in C57BL/6 and SJL mice. J. Immunol. 2007; 179:8470–8479. [PubMed: 18056394]
18. Engelhardt B, Kempe B, Merfeld-Clauss S, Laschinger M, Furie B, Wild MK, Vestweber D. P-selectin glycoprotein ligand 1 is not required for the development of experimental autoimmune encephalomyelitis in SJL and C57BL/6 mice. J. Immunol. 2005; 175:1267–1275. [PubMed: 16002731]
19. Naik SH, Proietto AI, Wilson NS, Dakic A, Schnorrer P, Fuchsberger M, Lahoud MH, O'Keeffe M, Shao QX, Chen WF, et al. Cutting edge: generation of splenic CD8$^+$ and CD8$^-$ dendritic cell equivalents in Fms-like tyrosine kinase 3 ligand bone marrow cultures. J. Immunol. 2005; 174:6592–6597. [PubMed: 15905497]
20. Dehlin M, Bokarewa M, Rottapel R, Foster SJ, Magnusson M, Dahlberg LE, Tarkowski A. Intra-articular fms-like tyrosine kinase 3 ligand expression is a driving force in induction and progression of arthritis. PLoS One. 2008; 3:e3633. [PubMed: 18982072]
21. Engelhardt B, Vajkoczy P, Laschinger M. Detection of endothelial/lymphocyte interaction in spinal cord microvasculature by intravital videomicroscopy. Methods Mol. Med. 2003; 89:83–93. [PubMed: 12958414]
22. Coisne C, Mao W, Engelhardt B. Cutting edge: natalizumab blocks adhesion but not initial contact of human T cells to the blood-brain barrier in vivo in an animal model of multiple sclerosis. J. Immunol. 2009; 182:5909–5913. [PubMed: 19414741]
23. Ley K, Gaehtgens P. Endothelial, not hemodynamic, differences are responsible for preferential leukocyte rolling in rat mesenteric venules. Circ. Res. 1991; 69:1034–1041. [PubMed: 1934331]
24. Von Andrian UH, Hansell P, Chambers JD, Berger EM, Torres Filho I, Butcher EC, Arfors KE. L-selectin function is required for β_2 integrin-mediated neutrophil adhesion at physiological shear rates in vivo. Am. J. Physiol. 1992; 263:H1034–H1044. [PubMed: 1384360]
25. Brasel K, De Smedt T, Smith JL, Maliszewski CR. Generation of murine dendritic cells from flt3-ligand-supplemented bone marrow cultures. Blood. 2000; 96:3029–3039. [PubMed: 11049981]
26. DeNucci CC, Pagán AJ, Mitchell JS, Shimizu Y. Control of $\alpha_4\beta_7$ integrin expression and CD4 T cell homing by the β_1 integrin subunit. J. Immunol. 2010; 184:2458–2467. [PubMed: 20118278]

27. Bullard DC, Hu X, Adams JE, Schoeb TR, Barnum SR. p150/95 (CD11c/CD18) expression is required for the development of experimental autoimmune encephalomyelitis. Am. J. Pathol. 2007; 170:2001–2008. [PubMed: 17525267]
28. Bailey SL, Schreiner B, McMahon EJ, Miller SD. CNS myeloid DCs presenting endogenous myelin peptides “preferentially” polarize $CD4^+$ T(H)-17 cells in relapsing EAE. Nat. Immunol. 2007; 8:172–180. [PubMed: 17206145]
29. Engelhardt B. The blood-central nervous system barriers actively control immune cell entry into the central nervous system. Curr. Pharm. Des. 2008; 14:1555–1565. [PubMed: 18673197]
30. Pendl GG, Robert C, Steinert M, Thanos R, Eytner R, Borges E, Wild MK, Lowe JB, Fuhlbrigge RC, Kupper TS, et al. Immature mouse dendritic cells enter inflamed tissue, a process that requires E- and P-selectin, but not P-selectin glycoprotein ligand 1. Blood. 2002; 99:946–956. [PubMed: 11806998]
31. Robert C, Fuhlbrigge RC, Kieffer JD, Ayehunie S, Hynes RO, Cheng G, Grabbe S, von Andrian UH, Kupper TS. Interaction of dendritic cells with skin endothelium: a new perspective on immunosurveillance. J. Exp. Med. 1999; 189:627–636. [PubMed: 9989977]
32. Cavanagh LL, Weninger W. Dendritic cell behaviour in vivo: lessons learned from intravital two-photon microscopy. Immunol. Cell Biol. 2008; 86:428–438. [PubMed: 18431356]
33. Allt G, Lawrenson JG. Is the pial microvessel a good model for blood-brain barrier studies? Brain Res. Brain Res. Rev. 1997; 24:67–76. [PubMed: 9233542]
34. Owens T, Bechmann I, Engelhardt B. Perivascular spaces and the two steps to neuroinflammation. J. Neuropathol. Exp. Neurol. 2008; 67:1113–1121. [PubMed: 19018243]
35. Barkalow FJ, Goodman MJ, Gerritsen ME, Mayadas TN. Brain endothelium lack one of two pathways of P-selectin–mediated neutrophil adhesion. Blood. 1996; 88:4585–4593. [PubMed: 8977250]
36. van Zwam M, Huizinga R, Melief MJ, Wierenga-Wolf AF, van Meurs M, Voerman JS, Biber KP, Boddeke HW, Höpken UE, Meisel C, et al. Brain antigens in functionally distinct antigen-presenting cell populations in cervical lymph nodes in MS and EAE. J. Mol. Med. 2009; 87:273–286. [PubMed: 19050840]
37. Yednock TA, Cannon C, Fritz LC, Sanchez-Madrid F, Steinman L, Karin N. Prevention of experimental autoimmune encephalomyelitis by antibodies against $\alpha_4\beta_1$ integrin. Nature. 1992; 356:63–66. [PubMed: 1538783]
38. Bartholomäus I, Kawakami N, Odoardi F, Schläger C, Miljkovic D, Ellwart JW, Klinkert WE, Flügel-Koch C, Issekutz TB, Wekerle H, Flügel A. Effector T cell interactions with meningeal vascular structures in nascent autoimmune CNS lesions. Nature. 2009; 462:94–98. [PubMed: 19829296]
39. del Pilar Martin M, Cravens PD, Winger R, Frohman EM, Racke MK, Eagar TN, Zamvil SS, Weber MS, Hemmer B, Karandikar NJ, et al. Decrease in the numbers of dendritic cells and $CD4^+$ T cells in cerebral perivascular spaces due to natalizumab. Arch. Neurol. 2008; 65:1596–1603. [PubMed: 18852339]
40. Stüve O, Marra CM, Jerome KR, Cook L, Cravens PD, Cepok S, Frohman EM, Phillips JT, Arendt G, Hemmer B, et al. Immune surveillance in multiple sclerosis patients treated with natalizumab. Ann. Neurol. 2006; 59:743–747. [PubMed: 16634029]

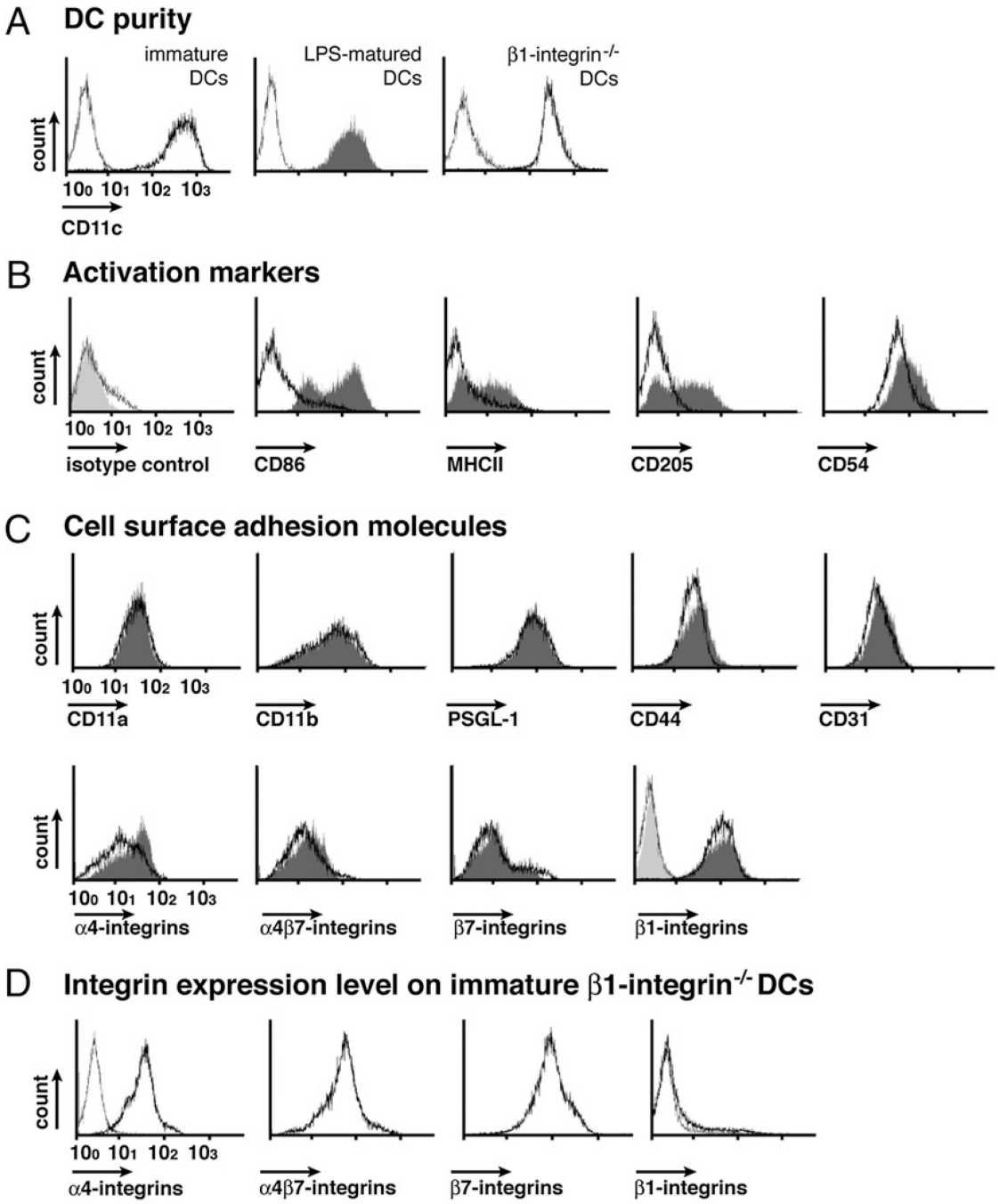

FIGURE 1.

Phenotype of Flt-3L–differentiated DCs *A*, Purity of immature DCs (black open histogram), LPS-matured DCs (dark gray filled histogram), and β_1 integrin$^{-/-}$ immature DCs (black open histogram) determined by cell surface staining for CD11c and FACS analysis is shown. *B* and *C*, Cell surface phenotype of immature DCs (black open histogram) was compared with the LPS-matured DCs (gray filled histogram) by FACS analysis. DC activation markers (*B*) and cell surface adhesion molecule expression (*C*) on immature (black open histograms) and LPS-matured (gray filled histograms) isolated from SJL mice are shown. The phenotype of immature DCs isolated from C57BL/6 mice was found to be indistinguishable. The *left top* histogram overlay shows rat IgG isotype control staining for immature (gray open histogram) and LPS-matured DCs (light gray filled

histogram), respectively. Hamster isotype control stainings are included in the overlay plot for β_1 integrins, which are detected by hamster antimouse-β_1 integrin Abs. *D*, Integrin expression levels on immature β_1 integrin$^{-/-}$ DCs (bold black open histogram). The *left* black open histogram overlay shows rat IgG isotype control staining for immature β_1 integrin$^{-/-}$ DCs. Hamster isotype control stainings are included in the overlay plot for β_1 integrins, which are detected by hamster anti–mouse-β_1 integrin Abs. Expression profiles are represented on a logarithmic scale in the *x*-axis. Results are representative of six experiments with similar results.

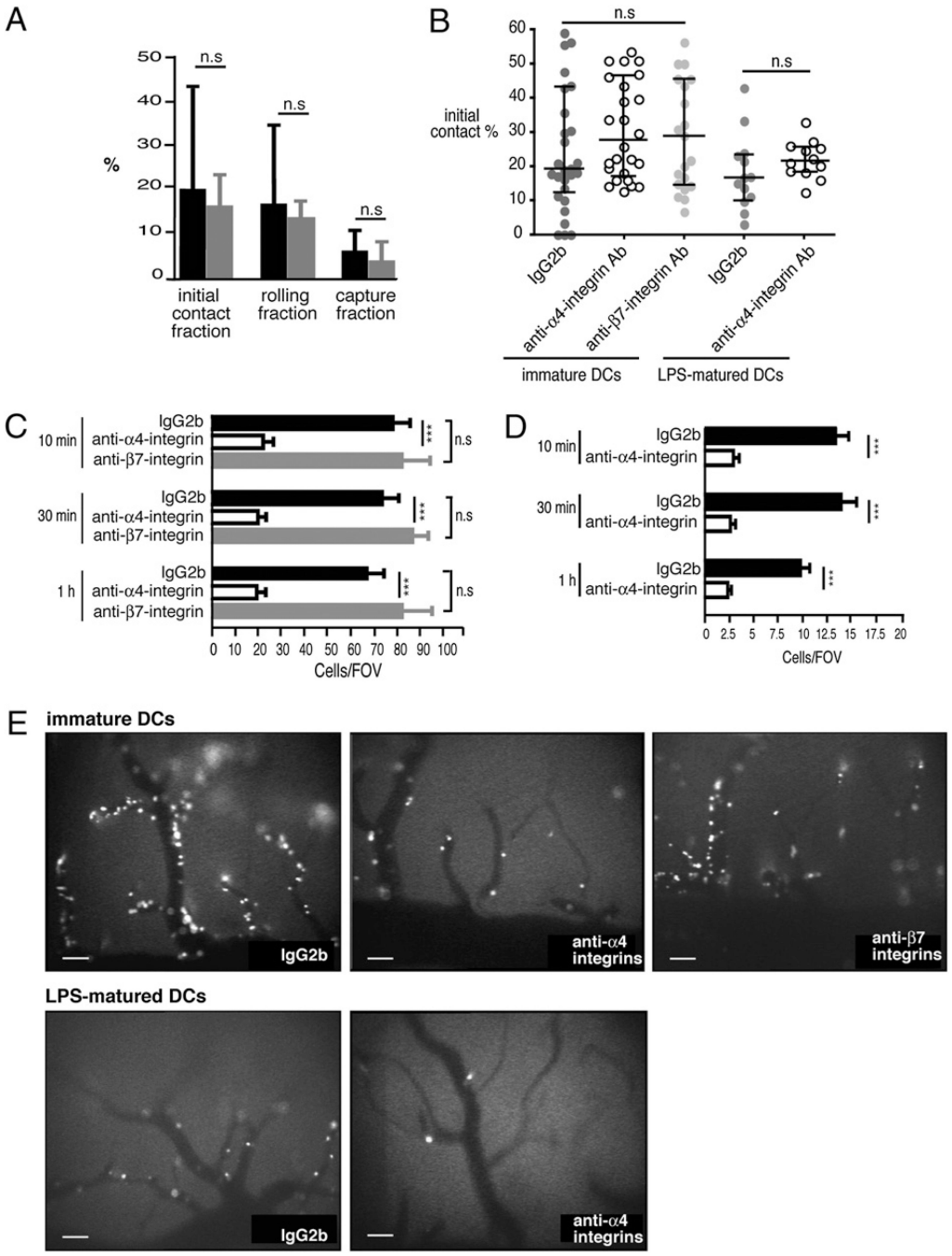

FIGURE 2.

Multistep DC interaction with the inflamed spinal cord microvascular wall during EAE. *A* and *B*, The fraction of DCs initiating contact with the vascular wall by rolling or capture was calculated for each postcapillary venule as the percentage of interacting DCs among the total number of DCs passing through a given microvessel during a 1 min recorded observation period. *A*, Initial contact, rolling and capture fraction of immature (black bars) and LPS-matured (gray bars) DCs treated with IgG2b isotype control mAb, within the spinal cord white-matter postcapillary venules. All values indicate medians with interquartile ranges of $n = 29$ analyzed postcapillary venules from seven mice for immature DCs and $n = 11$ postcapillary venules from four mice for LPS-matured DCs. *B*, Initial contact of immature DCs and LPS-matured DCs treated with either IgG2b isotype control mAb

(dark gray filled circles) or the anti-α_4 integrin mAb PS/2 (open circles) within the spinal cord white-matter postcapillary venules. Light gray filled circles indicate treatment of immature DCs with the anti-β_7 integrin mAb (Fib504). All values indicate medians with interquartile ranges of $n = 29$ analyzed postcapillary venules from seven mice for immature IgG2b-treated DCs, $n = 26$ postcapillary venules from five mice for anti-α_4 integrin mAb-treated DCs, $n = 21$ postcapillary venules from five mice for anti-β_7 integrin mAb-treated DCs, $n = 13$ analyzed postcapillary venules from four mice for LPS-matured DCs treated with IgG2b, and $n = 12$ analyzed postcapillary venules from three mice for LPS-matured DCs treated with the anti-α_4 integrin mAb PS/2. *C–E*, Permanently adherent DCs were defined as cells that attached to the vessel wall without moving or detaching from the endothelium for a period of 20 s and longer. *C* and *D*, Permanent DC adhesion at 10 min, 30 min, and 1 h after cell infusion was expressed as number of adherent DCs per FOV using the ×10 objective. Per mouse, four to six FOVs can be defined within the spinal cord window. The numbers of firmly adherent DCs per FOV from different mice were pooled to generate a mean ± SEM. Firm adhesion of immature DCs (*C*, black bars) and LPS-matured DCs (*D*, black bars), treated with IgG2b isotype control mAb, to the BBB endothelium at different time points after cell infusion is shown. Treatment with the anti-α_4 integrin mAb PS/2 significantly reduced adhesion of immature DCs (*C*, open bars) and LPS-matured DCs (*D*, open bars) to the inflamed spinal cord white-matter BBB. In contrast, treatment of immature DCs with the anti-β_7 integrin mAb Fib504 had no effect (*D*, gray bars). The number of mice included in these analyses per group: immature DCs, IgG2b isotype control, $n = 7$, PS/2, $n = 5$, and Fib504, $n = 4$; and LPS-matured DCs, IgG2b control, $n = 5$ and PS/2, $n = 3$. All values are means ± SEM. Mann-Whitney *U* test was used to evaluate statistical significance. $*p < 0.05$; $**p < 0.01$; $***p < 0.001$. *E*, Video snapshots from one representative FOV per condition visualizing the firmly adherent DCs within the spinal cord white-matter microvasculature at 10 min after cell infusion. Scale bars, 100 μm. FOV, field of view.

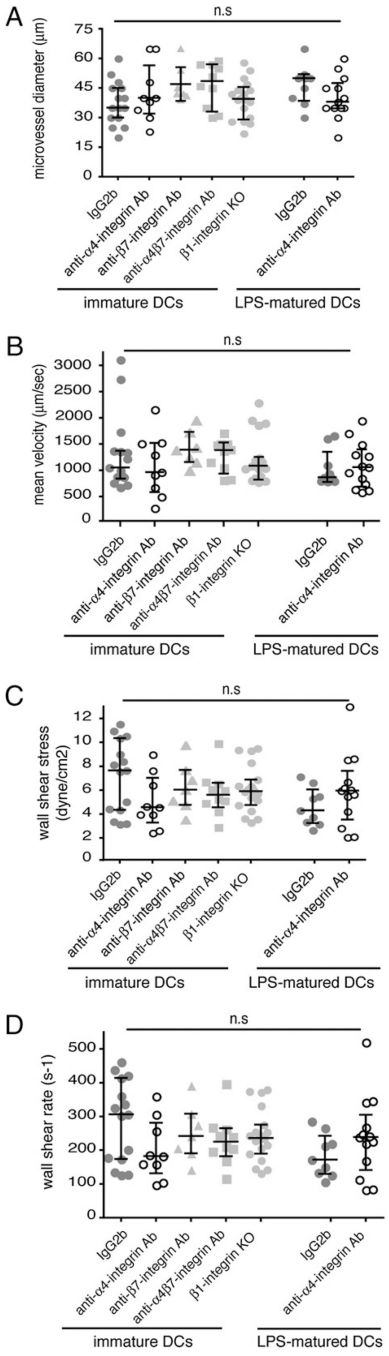

FIGURE 3.

Microhemodynamic parameters in the postcapillary venules of the inflamed spinal cord white matter in SJL mice with $PLP_{aa\ 139–151}$-induced EAE. Hemodynamic parameters were determined in three to four mice per group in the indicated number of postcapillary venules. For immature DCs, IgG2b isotype control, *n* = 15 venules; PS/2, *n* = 9; Fib504, *n* = 7 venules; β_1 integrin$^{-/-}$, *n* = 19; and DATK32, *n* = 10 venules. For LPS-matured DCs, IgG2b isotype control, *n* = 9 venules and PS/2, *n* = 13 venules. *A*, Microvessel diameters in micrometers. *B*, Mean blood flow velocity (micrometers per second). *C*, Wall shear rate (s^{-1}). *D*, Wall shear stress (dyne/cm). Each dot represents one analyzed postcapillary venule. Quantitative data are given as medians with interquartile ranges. Statistical significance was determined by the Mann-Whitney *U* test.

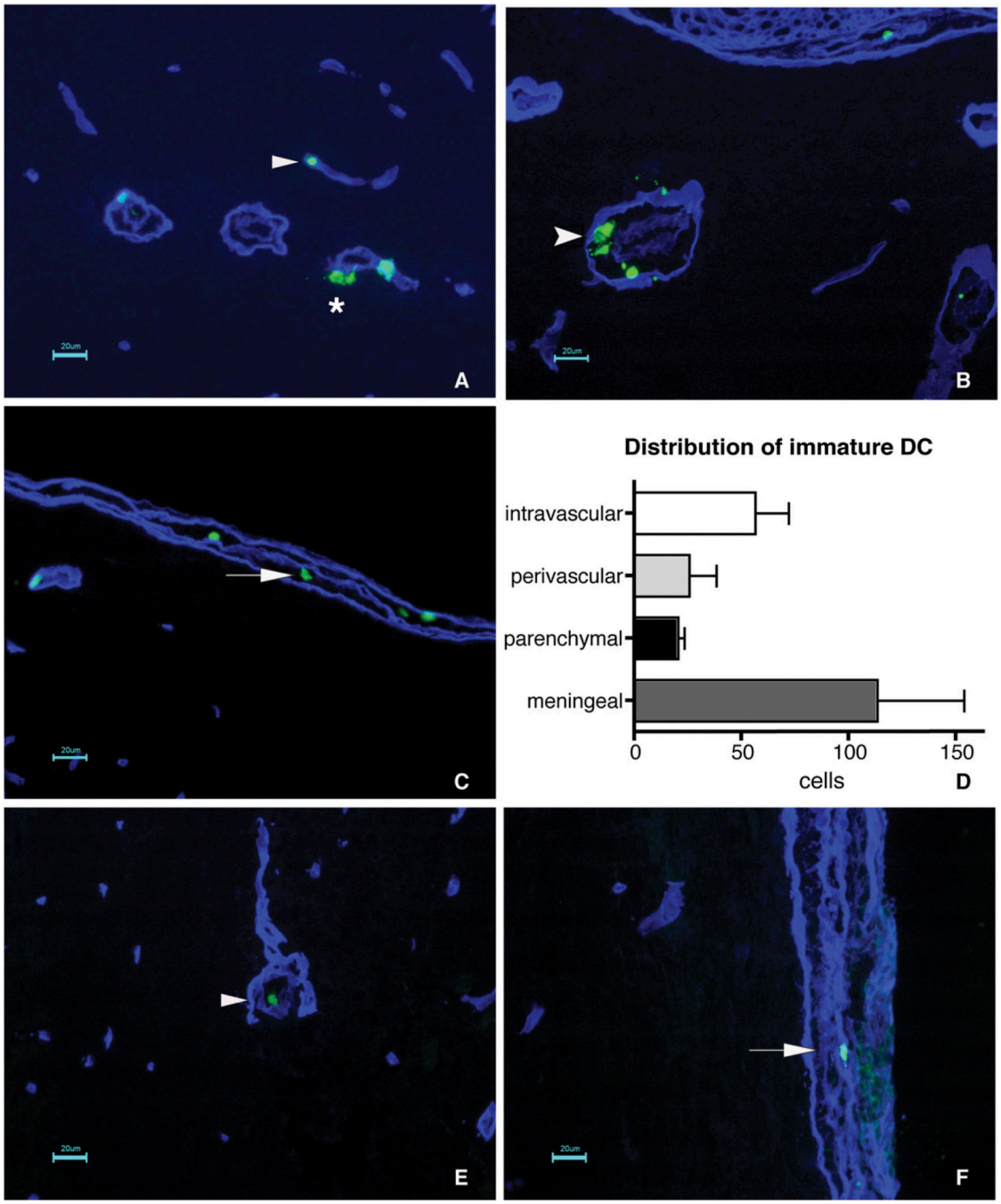

FIGURE 4.

Immature but not mature DCs migrate across parenchymal CNS microvessels during EAE. *A–C*, Distribution of immature DCs in spinal cord tissue sections of SJL mice with EAE 3 h postinfusion is shown. A laminin staining (blue) was performed to distinguish the endothelial and parenchymal basement membranes, defining the inner and outer borders of the perivascular space around CNS microvessels. Cell Tracker green-labeled DCs are detected intravascularly (*A*, arrowhead) or beyond the basement membranes within the CNS parenchyma (*A*, star) as well as within the perivascular space of inflamed spinal cord microvessels (*B*, feathered arrowhead), demonstrating that immature DCs can enter the CNS parenchyma via parenchymal micro-vessels. Nevertheless, the majority of immature DCs was found dispersed throughout the meningeal compartment (*C*, arrow), suggesting

that the majority of immature DCs enters the CNS via this route. *D* depicts the quantitative analysis of the distribution of immature DC within the CNS as detected 3 h after infusion. Bars represent the mean ± SEM of three sections per mouse. A total of three mice were analyzed. Statistical analysis using unpaired two-tailed Student *t* test showed no significant differences between the groups. *E* and *F*, Rare LPS-matured DCs could be detected in spinal cord tissue sections of SJL mice with EAE 3 h after infusion. LPS-matured DCs were found to be strictly confined to the circulation (*E*, arrowhead) or to the meningeal compartment (*F*, arrow). Scale bars, 20 μm.

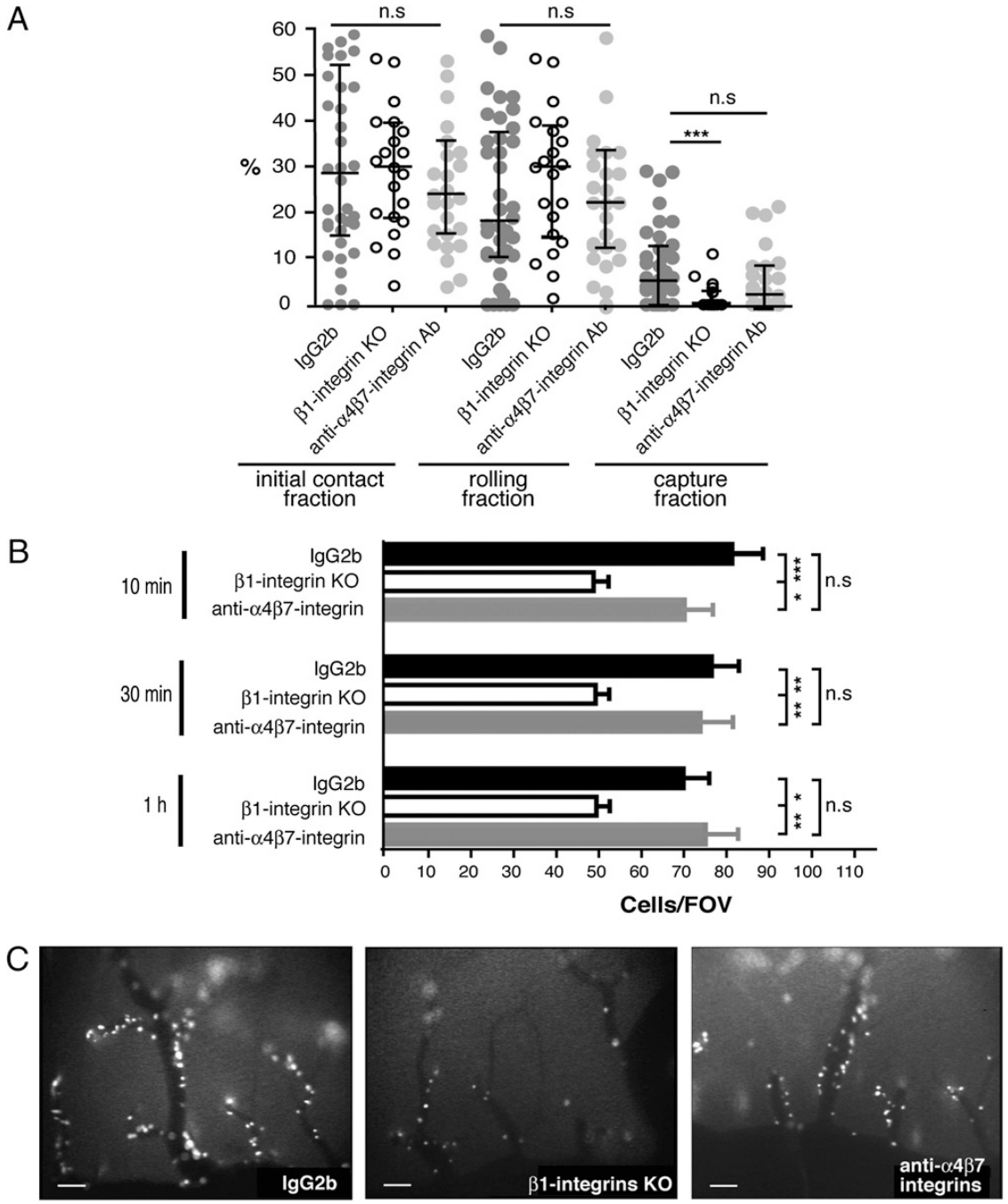

FIGURE 5.

Involvement of $\alpha_4\beta_1$ versus $\alpha_4\beta_7$ integrin in the multistep interaction of immature DCs with the inflamed spinal cord microvascular wall during EAE. *A*, The fraction of DCs initiating contact with the vascular wall by rolling or capturing was calculated for each postcapillary venule as the percentage of interacting DCs among the total number of DCs passing through a given microvessel during a 1-min recorded observation period. Initial contact, rolling and capture fraction of immature DCs treated with either IgG2b isotype control mAb (dark gray filled circles) or the anti-$\alpha_4\beta_7$ integrin mAb DATK32 (light gray filled circles) or immature β_1 integrin$^{-/-}$ DCs (open circles) within the spinal cord white-matter postcapillary venules. All values indicate medians with interquartile ranges of n = 39 analyzed postcapillary venules from nine mice infused with immature

IgG2b-treated DCs from both SJL and C57BL/6 mice, $n = 21$ postcapillary venules from five mice infused with anti-$\alpha_4\beta_7$ integrin mAb-treated DCs from both SJL/J and C57BL/6 mice, and $n = 27$ postcapillary venules from five mice infused with β_1 integrin$^{-/-}$ DCs. Mann-Whitney *U* test was used to evaluate statistical significance. *$p < 0.05$; **$p < 0.01$; ***$p < 0.001$. *B*, Permanent DC adhesion at 10 min, 30 min, and 1 h after DC infusion were expressed as number of adherent DCs per field of view (FOV) using the ×10 objective. Firm adhesion of immature DCs (black bars) treated with IgG2b isotype control mAb to the inflamed BBB endothelium at different time points after cell infusion is shown. The adhesion of immature β_1 integrin$^{-/-}$ DCs to the inflamed spinal cord white-matter BBB was significantly reduced (open bars), whereas blocking $\alpha_4\beta_7$ integrin had no effect on the adhesion of immature DCs (gray bars). The numbers of firmly adherent DCs per FOV from different mice were pooled. Number of mice included in these analyses per group: immature DCs, IgG2b control, $n = 11$; DATK32, $n = 5$; and β_1 integrin$^{-/-}$, $n = 11$. All values are means ± SEM. *$p < 0.05$; **$p < 0.01$; ***$p < 0.001$. Statistical significance was determined by the Mann-Whitney *U* test. *C*, Video snapshots from one representative field of view per condition visualizing the adhesion of DCs within the spinal cord white-matter microvasculature are shown at 10 min after cell infusion. Scale bars, 100 μm.